doi. 10.39429/ace.v814.37/3

ORIGINAL RESEARCH ARTICLE

Synthesis of CoCrNiOx high entropy oxide catalyst and its oxidative desulfurization performance

Muntasser Sahib Taha1*, Hameed Hussein Alwan1

Chemical Engineering Department, College of Engineering, University of Babylon, Hilla, 51002, Iraq

*Corresponding author: Muntasser Sahib Taha; eng176.muntasser.sahib@student.uobabylon.edu.iq

ABSTRACT

The production of ultraclean fuel represents a big challenge for scientists and workers in the petroleum industry because the presence of sulfur in the fuel may have severe consequences for human health and the environment. Oxidative desulfurisation (ODS) is a promising technology when compared with classical hydrodesulfurisation (HDS). In this work, the production of a new catalyst for the ODS process, in which a mixed oxide catalyst was synthesised by mechanochemistry mixing of three metal chlorides (cobalt, nickel, and chromium chlorides), and the atmospheric oxygen was used as an oxidant agent for Iraqi gasoil desulfurisation in an aerobic oxidative desulfurisation (AODS). The prepared catalyst was characterised by X-ray diffraction (XRD), Fourier transform infrared spectroscopy (FTIR), scanning electron microscopy (SEM), and Energy Dispersive X-ray analysis (EDX). The study included an investigation of the effect of catalyst dosage, reaction temperature, and oxidation time. Response surface methodology (RSM) was used to investigate the performance of the AODS reaction and to evaluate the main impact of the studied variables, as well as the interaction and quadratic effects, for determining the optimum condition. According to the findings obtained from the regression analysis, the experimental data were fitted to a quadratic model with a high correlation coefficient (R² 0.9839), adjusted correlation coefficient (Adj. R2 0.9419), and predicted correlation coefficient (Pred. R2 0.7419). The AODS process was applied with a maximum sulfur removal efficiency of 99% under operating conditions of 0.75 g catalyst dosage, 200 °C reaction temperature, and 60 minutes reaction time. The experimental sulfur removal efficiency was in satisfactory agreement with the predicted efficiency of 98.12%. Analysis of variation (ANOVA) shows that oxidation time is the most significant factor affecting sulfur removal efficiency, followed by reaction temperature and catalyst dosage, as indicated by their F-values.

Keywords: Dibenzothiophene; oxidation; Box- Behnken experimental design; fuel, desulfurisation

ARTICLE INFO

Received: 18 September 2025 Accepted: 15 October 2025 Available online: 20 October 2025

COPYRIGHT

Copyright © 2025 by author(s). Applied Chemical Engineering is published by Arts and Science Press Pte. Ltd. This work is licensed under the Creative Commons Attribution-NonCommercial 4.0 International License (CC BY 4.0).

https://creativecommons.org/licenses/by/4.0/

1. Introduction

Crude oil is a complex mixture of different hydrocarbon compounds. In addition to hydrogen and carbon, it contains sulfur, nitrogen, and oxygen, as well as other metal compounds. In which sulfur compounds may take different forms, such as sulfides, disulfides, mercaptans, and thiophene [1]. The sulfur compounds will produce sulfur oxides when the fuel is combusted, which are responsible for environmental pollution and have adverse effects on human health. Additionally, the presence of sulfur components causes metallic equipment corrosion and catalyst poisoning that is used in the upstream unit, e.g., valuable platinum catalysts in the catalytic reforming unit [2], therefore, the countries' governments were issued an environmental regulation that limited the allowable sulfur content associated with the different types of fuel for example, the Chinese government limits the

sulfur content below 10 ppm according to the Chinese national V standard [3].

The most common technique used to remove sulfur compounds from fuel is the hydrodesulfurisation (HDS) method. The HDS method can remove many forms of sulfur compounds. Still, it requires significant energy and effort to remove some refractory compounds, such as high molecular weight thiophen derivatives like benzothiophene (BT) and dibenzothiophene (DBT). On the other hand, the HDS method requires operation at elevated temperature and pressure, which involves consuming a huge amount of hydrogen gas ^[1,4]. Oxidative desulfurisation (ODS) may be considered a promising alternative technique for moving refractory sulfur compounds.

Furthermore, it works at moderate operating conditions (relatively low pressure and temperature), and it is characterised by its selectivity; it does not need to provide expensive hydrogen, as in the HDS method. During ODS, the sulfur compounds are oxidised into corresponding sulfoxides and sulfones, depending on the oxidant and catalyst used ^[4]. Commonly, oxygen O2 ^[5], hydrogen peroxide H2O2, and tetra-Butyl hydroperoxide (TBHP) ^[6] are used as oxidant agents in the ODS process. Still, among them, oxygen has an advantage due to its availability, low cost, and relatively high safety, so it is often considered an ideal oxidant agent.

The ODS process is a catalytic reaction, which means a catalyst is required s0, so there are Many catalytic systems applied in the ODS process, for instance, polyoxometalate (POM) ^[7], ionic liquid ^[8], metal-organic frameworks ^[9], metal ^[10], and metal oxide, and so on. Most of which were conducted by using metal oxide supported on a suitable support, especially transition metal-based catalysts (Vanadium, Titanium, molybdenum, etc) have attracted much attention for deep desulfurisation, for instance, Cerium supported on Al2O3 ^[11], Iron (III) oxide supported on graphene ^[12], CuO/SiO2 and CuO/TiO2-SiO2 nano catalysts ^[13], cerium–tungsten catalyst supported on activated carbon ^[14], etc.

Although the metal-supported catalysts have high activity, they are easy to agglomerate and sinter at high temperatures. Of late, entropy-stable, disordered, and energy-stable metal oxide catalysts have been reported. These catalysts consist of five or more metal elements, which are characterised by a single-phase metal oxide formed at high temperature from the different crystal structures of metal oxides because of the similar atomic size of the resource metal [15]. Furthermore, the formation of a solid solution is beneficial for the dispersion of all elements, which enhances the dispersion of catalytically active sites. Compared to conventional metal oxides, their high-entropy structures create structural defects that are often suitable for acting as catalytically active sites. These advantages pave the way for the use of high-entropy oxides to prepare catalysts, enhancing catalytic performance. The investigations show that the atomic size and enthalpy of mixing are important parameters that affect the solid solution of high entropy oxides (HEO) [16], so the mixture's Gibbs free energy $\Delta G_{mix} = \Delta H_{mix}$ -T ΔS_{mix} to estimate the phase stability for high-entropy systems, and to obtain a high entropy structure under moderate conditions by decreasing the mixing enthalpy [17].

In this study, we reported a high entropy oxide (HEO) catalyst, CoCrNiOx, synthesised by mechanochemistry mixing of their chlorides. The chosen metals are characterised by their high activity for oxidation reactions. The prepared catalyst was used in the aerobic oxidative desulfurisation (AODS) of Iraqi gas oil, demonstrating the catalytic activity of the HEO catalyst under three operating parameters: catalyst dosage, reaction temperature, and oxidation time. Hence, developing the AODS process using the CoCrNiOx catalyst can be considered a promising new research direction for sulfur removal from transportation fuel (specifically, gasoil). Since most of the previous studies are based on a time technique, in the present work, response surface methodology (RSM) was used to estimate the main impact of the studied parameters, their synchronised interactions, and quadratic effects to reach the optimum operating condition for the AODS process.

2. Experimental method

2.1. Feedstock

Iraqi gas oil (specific gravity 0.8406) supplied from the Al-Najaf refinery was used as a feedstock. **Table** 1 shows ASTM distillation data for the used gas oil. The additional data includes a viscosity of 3.2 cSt at 40°C, a flash point of 94.5°C, an ash content of 0.002%, and a cetane index of 56.1.

Table 1. Gas oil ASTM distillation data

Vol.%	0	10	20	30	40	50	60	70	80	90	100
Temp (°C)	225	246	253.2	260	267	275.5	285.3	297.7	314.7	314.7	367

The total sulfur content is 1.5 wt.%, Total sulfur concentration is expressed without going into details of the sulfur compounds present.

2.2. Chemicals

cobalt (II) chloride (CoCl₂.6H₂O - Merck 99%), nickel (II) chloride (NiCl₂.6H₂O - Sigma-Aldrich 98%), chromium (III) chloride (CrCl₃.H₂O - Alfa Chemika 99%), are utilised as precursors for cobalt, nickel, and chromium oxides. Acetonitrile (CH₃CN, Sigma-Aldrich, 99.9%). Atmospheric oxygen as an oxidation agent.

2.3. Catalyst preparation

The catalyst was made by mixing equal amounts of all metal chlorides (0.0025 mol each) and 0.125 mol of urea using a mechanical process. The mixture was loaded into a ball mill, equipped with 7 mm ceramic balls, and mixed at a rotational speed of 400 rpm for 2 hours to facilitate thorough mixing and grinding. Transferring the mixture into a desiccator at 80°C overnight reduced the moisture content [18]. The obtained paste was subjected to calcination at 700°C for 3 hours using an electric furnace (JINYU model 1700). The synthesised catalyst was evaluated using X-ray diffraction (XRD) and Fourier transform infrared spectroscopy (FTIR).

2.4. AODS reaction and solvent extraction

The effectiveness of the catalyst was tested using the AODS reaction in a lab-scale reactor, with a 250 mL three-neck flask serving as the reactor (containing 100 mL of gas oil). The three openings in the flask serve the following purposes: the first is designated for air entrance, the second neck opening was equipped with a total reflux condenser to reflux the evaporated gas oil, and the third opening is utilised for the insertion of the catalyst and feedstock, as well as for the suction of the products. The reactor temperature was monitored and controlled by inserting a type-K thermocouple inside the reactor. The thermocouple was linked to the OMRON E5C4-R20K temperature controller, which has a temperature range of 0–400°C, while the reactor (flask) was heated using a water bath.

The catalyst performance was investigated in relation to three operating parameters: catalyst dosage, reaction temperature, and oxidation time. The Box-Behnken experimental design (BBD) combination with response surface methodology (RSM) was applied for analysis and optimisation of the experimental conditions using Design Expert ver. 13 software. In this work, the BBD was used for an investigation of the impact of three parameters on sulfur removal efficiency, in which the BBD design consists of three blocks, in each of which two parameters are varied through four possible combinations of low and high levels, plus a centre point (we used two repeated points). The levels of each parameter studied are presented in **Table 2**.

Table 2. Experimental design levels of chosen variables studied.

Variables (anis)	Country of the DDD	levels			
Variables (unit)	Symbol in BBD	-1	0	1	
Catalyst dosage (g / mL 100)	A	0.5	0.75	1.0	
Reaction Temperature (°C)	В	150	175	200	
Oxidation time (minutes)	C	30	45	60	

The experimental data from BBD were analysed and fitted into a second-order (quadratic) polynomial model as the equation below:

$$Y = \beta_0 + \sum_{i=1}^{n} \beta_{iX_i} + \sum_{i=1}^{n-1} \sum_{j=1+1}^{n} \beta_{ij} X_i X_j + \sum_{i=1}^{n} \beta_{ii} X_i^2$$
 (1)

where Y represents the response (final sulfur concentration), $\beta 0$ represents the constant term. The variables Xi and Xj mean the coded values of the studied parameters, with βi , βii , and βij signifying the linear, quadratic, and interaction coefficients, respectively [19].

The operational parameters (amount of catalyst, temperature, and time) were changed based on the BBD experimental design, as shown in **Table 3**. The feedstock was introduced into the reactor, and heating commenced until the required temperature was achieved. The designated quantity of catalyst was introduced into the reactor, and air was subsequently fed at a flow rate of 20 L/min, initiating the reaction, which was stopped upon reaching the time ascribed according to the BBD matrix. The reaction product was suctioned for the second step (solvent extraction step), where it was mixed with acetonitrile (solvent) in a lab-scale shaker (ORBITAL Shaker, Rotator Model VRN-480 from GEMMY Industrial Corp.) for 30 minutes at 100 rpm and laboratory temperature. The mixture was separated into two layers based on density differences when poured into a separation funnel and left to settle. Two layers have developed within the separation funnel; the upper layer consists of low-sulfur fuel, whereas the lower layer comprises sulfones and solvent (oxidation products and acetonitrile). The final sulfur content was measured with the X-ray fluorescence sulfur analyser (SPECTROSCAN SL TU 4276-002-23124704). The following equation determines the sulfur removal efficiency:

$$R\% = \frac{Si\text{-}So}{Si} \times 100 \tag{2}$$

Where (Si) is the initial sulfur concentration, and (So) is the final sulfur concentration.

Table 3. Experimental design matrix generated by applying BBD, and experimental response with real value for the operating conditions for all runs

		Coded value					
Run	Factor 1 A catalyst dosage)	Factor 2 B (reaction Temperature)	Factor 3 C(oxidation time)	Factor 1 A catalyst dosage)	Factor 2 B (reaction Temperature)	Factor 3 C (oxidation time)	R%
1	-1	-1	0	0.5	150	45	71
2	1	-1	0	1	150	45	67
3	-1	1	0	0.5	200	45	85
4	1	1	0	1	200	45	79
5	-1	0	-1	0.5	175	30	58
6	1	0	-1	1	175	30	53
7	-1	0	1	0.5	175	60	84
8	1	0	1	1	175	60	80
9	0	-1	-1	0.75	150	30	62
10	0	1	-1	0.75	200	30	73

		Coded value					
Run	Factor 1 A catalyst dosage)	Factor 2 B (reaction Temperature)	Factor 3 C(oxidation time)	Factor 1 A catalyst dosage)	Factor 2 B (reaction Temperature)	Factor 3 C (oxidation time)	R%
11	0	-1	1	0.75	150	60	76
12	0	1	1	0.75	200	60	99
13	0	0	0	0.75	175	45	75
14	0	0	0	0.75	175	45	75

Table 3. (Continued)

3. Results and discussion

3.1. Catalyst characterisation

Figure. 1 illustrates the FTIR spectra of the prepared catalyst. In the FTIR spectra, the stretching vibration band corresponds to O—H (3441 cm ⁻¹), indicating the presence of a hydroxyl group and adsorbed water molecules ^[20], stretching C—H vibration around (2980-2930 cm ⁻¹) demonstrates aliphatic structure, the peak at close to 1735 cm ⁻¹, confirms the presence of (C=C) band, indicating the existence of a carboxyl group, which is included in aldehydes, ketones, and carboxylic acids. The band at 1380 cm ⁻¹ suggests the existence of O—H, signifying a phenolic group ^[21] There is a band at approximately 1288 cm ⁻¹ which represents C—O ^[22]. Some peaks appear at 400 – 800 cm ⁻¹, corresponding to the metals—oxygen (M—O) vibration, where the band around 570 cm ⁻¹ is attributed to cobalt-oxygen (Co—O), while the band near 660 cm ⁻¹ corresponds to the connecting vibration of cobalt-oxygen-cobalt (Co—O—Co)^[22] the peaks around 980 cm ⁻¹ can be assigned to chromyl (Cr=O) vibrations^[23]. The broad absorption band in the region of 700-600 cm ⁻¹ is ascribed to the stretch vibration of nickel-oxygen ^[24].

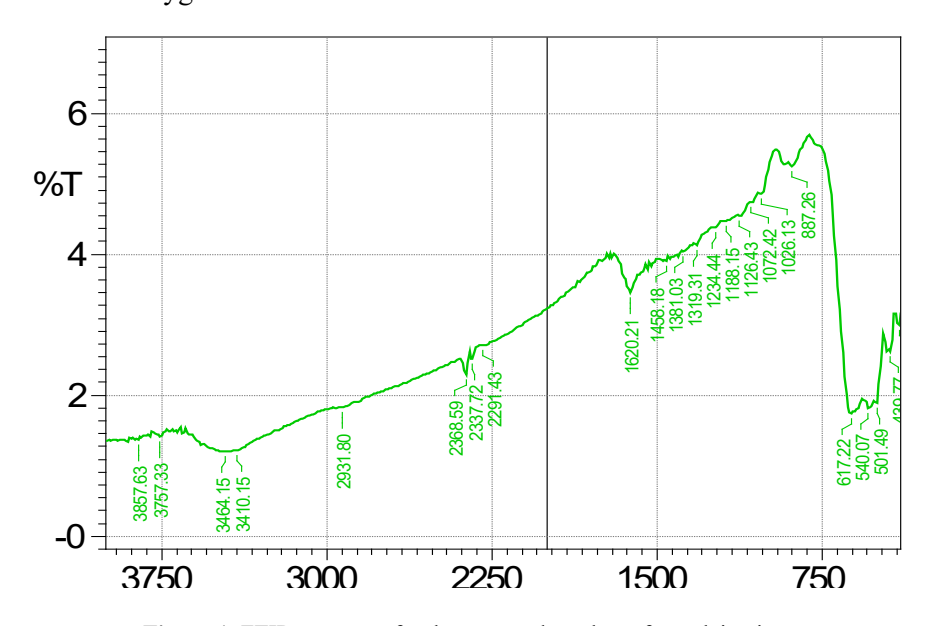


Figure 1. FTIR spectrum for the prepared catalyst after calcination

The pattern attained from XRD analysis for the synthesised catalyst is shown in **Figure 2**. As seen, the three metals are entirely incorporated into a supersaturated structure at the designated calcination temperature of 700 °C. The distinct peaks were observed at 2θ values of approximately 35.6 and 43.1, corresponding to 111 and 200 planes, respectively, which indicates that the cubic cobalt oxide production involves a peak at 35.64, attributed to cobalt oxide with a face-centred cubic (FCC) structure [25]he peak at 62.02 ° is assigned to the presence of nickel oxide [27], whereas the peaks at 36.74 and 53.76 ° indicate the presence of chromium oxide [26].

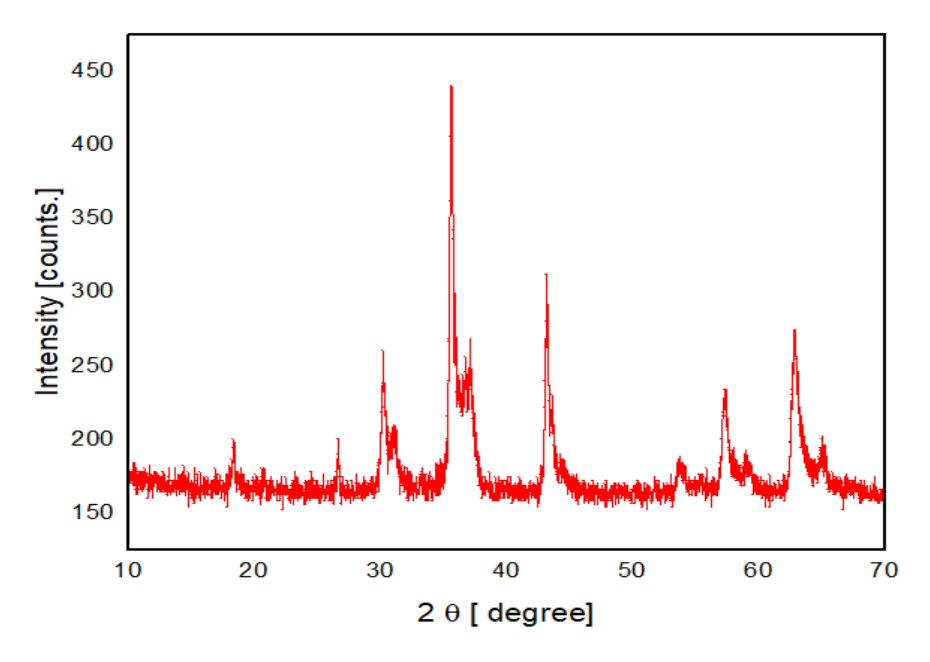


Figure 2. X-ray diffraction pattern for the prepared catalyst. The pattern was analysed by comparison with previous literature [27-29]

The aggregation of particles is a crucial factor in the crystallisation of metal oxides. The elemental composition of the synthesised catalyst was ascertained using EDS analysis. Figure 3. shows the EDS spectra, demonstrating the measurements of three elements, including oxygen, which serves as compelling evidence for the creation of metal oxides. The presence of metals (nickel, chromium, and cobalt) utilised for catalyst synthesis is acknowledged; however, their weight percentages deviate from the intended values, indicating undesirable agglomeration in certain areas of the catalyst surface, as evidenced by the SEM image. These findings affirm the successful integration of metals into the catalyst surface. The difference between what was found and what was expected was due to the technique used for catalyst synthesis, as well as other parameters such as surface oxidation, contamination, and the sticking of different elements, which could cause this gap.

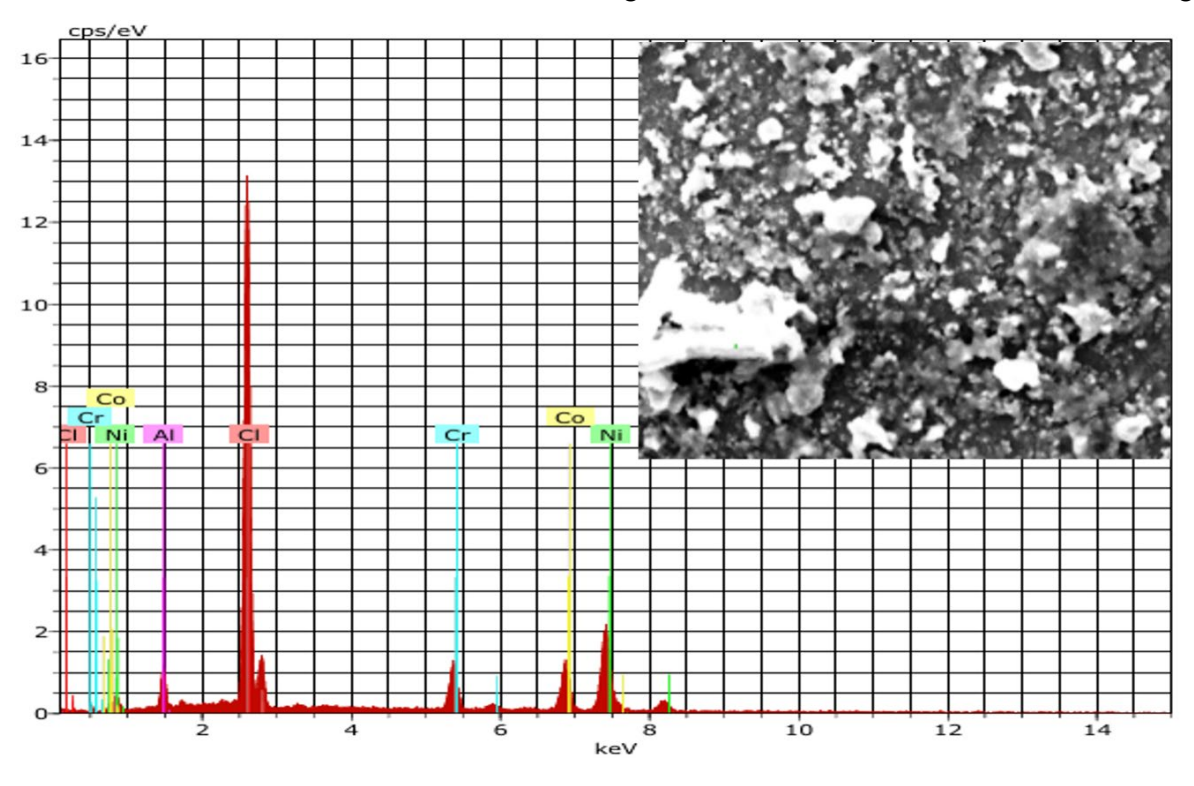


Figure 3. EDS result for the prepared catalyst showing the elemental distribution

4. AODS Catalytic reaction performance

4.1. RSM approach and ANOVA analysis

Response surface methodology is used to evaluate the main impact of the parameters studied, their combined impact, and the quadratic model impact to conduct the optimisation conditions. Experimental data (shown in **Table 3**) were fitted to the second-order polynomial(quadratic) model to get the regression equation. The model in terms of coded factors is:

$$R\% = 74.50 - 0.125 A + 7.12 B + 9.75 C - 2.37 A^{2} + 2.63 B^{2} + 0.375 C^{2} + 0.25 AB - 3.50 AC + 3.0BC$$
(6)

According to **Table 5**, the ANOVA study suggested that the second-order polynomial was highly significant with a 95% confidence level and an F-value of 15.54. The correlation coefficient R² is 0.9839, and the adjusted correlation coefficient (Adj. R²) is 0.9419. They are quite close to each other; moreover, the difference between Adj. The R² and predicted R² (Pred. R²) of 0.7419 are 0.205 (relatively acceptable), indicating a good agreement between the actual data and model-predicted values [27]. The obtained amount of 19.744 for adequate precision (more than 4) means a satisfactory signal-to-noise ratio.

4.2. Optimal operating conditions for sulfur removal efficiency

To achieve the maximum sulfur removal efficiency, the optimum values of the studied parameters were presented to Design Expert 13 software. The predicted sulfur removal efficiency from the results analysis shows that the optimum value is 98.12% at a catalyst dosage of 0.75 g, a reaction temperature of 200 °C, and an oxidation time of 60 minutes, while the actual value is 99%. There is a satisfactory agreement between the actual (obtained from experiments) and predicted values (estimated by the quadratic model).

Source	DF	Sum of Squares	Mean of Squares	F-Value	P-Value
Model	9	1783.68	198.19	27.10	0.0031
Dosage	1	45.13	45.13	6.17	0.0679
Temperature	1	450.00	450.00	61.54	0.0014
Time	1	1081.12	1081.12	147.85	0.0003
Dosage*Dosage	1	54.45	54.45	7.45	0.0525
Temperature*Temperature	1	68.45	68.45	9.36	0.0377
Time*Time	1	14.45	14.45	1.98	0.2325
Dosage*Temperature	1	1.000	1.000	0.1368	0.7303
Dosage*Time	1	0.2500	0.2500	0.0342	0.8623
Temperature*Time	1	36.00	36.00	4.92	0.0525
Lack-of-Fit	3	29.25	7.31		
Pure Error	1	0.0000	0.000		
Total	13	1812.93			

Table 4. ANOVA results for the second-order polynomial model for sulfur removal efficiency.

4.3. Impact of the studied variables

The value of the intercept coefficient ($\beta 0 = 74.5$) represents the average value of the sulfur removal efficiency when all parameters are fixed at their centre point values. In contrast, the magnitude of other coefficients for each term indicates the degree of importance of that term. According to the F-value, the most influential factors among the main terms were the oxidation time, followed by the reaction temperature and the catalyst dosage, with F-values of 147.85, 61.54, and 6.17, respectively.

The activity of the prepared catalyst for sulfur removal from gas oil via the AODS reaction is evaluated under three operational parameters: catalyst dosage, reaction temperature, and oxidation time. This study aims to explain how these factors affect sulfur removal, with the separate impacts of each variable illustrated in **Figure 4**. The removal of sulfur increased with elevated reaction temperature and prolonged oxidation duration. In contrast, it diminished with an increase in catalyst dosage. The rise in catalyst quantity results in enhanced sulfur removal, possibly due to the increased availability of active sites that facilitate the reaction [14]. However, sulfur removal efficiency does not continue to increase with the augmentation of catalyst quantity, as it begins to decline after reaching its maximum value. This phenomenon may be attributed to the accumulation and agglomeration of catalyst particles, which reduces the number of active sites on the catalyst surface [27, 28]. The results indicated that sulfur removal increased with rising reaction temperature, demonstrating that temperature is a crucial factor for improving ODS reaction efficacy. The improvement in sulfur removal as the reaction temperature goes up is due to how temperature affects the rate of oxidation reactions, according to the Arrhenius equation. This elevation in temperature improves sulfur removal efficiency.

Additionally, the rise in reaction temperature increases the number of reactant molecules possessing adequate activation energy, thereby facilitating oxidation interaction among the reactants. The improvement in sulfur removal as the reaction temperature goes up is due to how temperature affects the rate of oxidation reactions, according to the Arrhenius equation. This elevation in temperature improves sulfur removal efficiency. Additionally, the rise in reaction temperature increases the number of reactant molecules possessing adequate activation energy, thereby facilitating oxidation, which is the reaction among the reactants [30]. Raising the reaction temperature helps mix the reactants better. It spreads them out, making it easier for them to interact with the active sites in the catalyst pores [31]. Additionally, temperature affects the number of acidic centres in the catalyst structure, which in turn influences the catalyst's properties that improve AODS efficiency [28].

The results showed that removing sulfur is more effective when air is used as an oxidation medium. The presence of molecular oxygen (O_2) in the air is what improves this. It helps oxidise organosulfur compounds (OSCs) into sulfoxides and sulfones, which are more polar and easier to extract. Adding air facilitates interaction between the oxidant and OSCs by increasing the amount of oxygen and mass transfer, thereby improving the oxidative desulfurisation (AODS) process. Murata et al $^{[32]}$ have found that utising air as a mild oxidant helps thiophenic compounds convert more effectively, especially when the temperature and pressure are just right. It's important to note, though, that while using air is helpful, being exposed to it for a long period or too much aeration might cause sulfur removal efficiency to level off or even drop somewhat. This is because dissolved oxygen doesn't stay in the solution for as long, and the oxidant may not work as well. The study that looked at air and cobalt phthalocyanine in an ionic liquid medium showed that the conversion of dibenzothiophene (DBT) went up with the flow rate of air up to about 100 mL/min, but then went down at higher flow rates because there wasn't enough time for oxygen to react with the solution, which made oxidation less effective $^{[33]}$. Therefore, to maximise the effectiveness of AODS, it is crucial to ensure optimal airflow rate and reaction conditions.

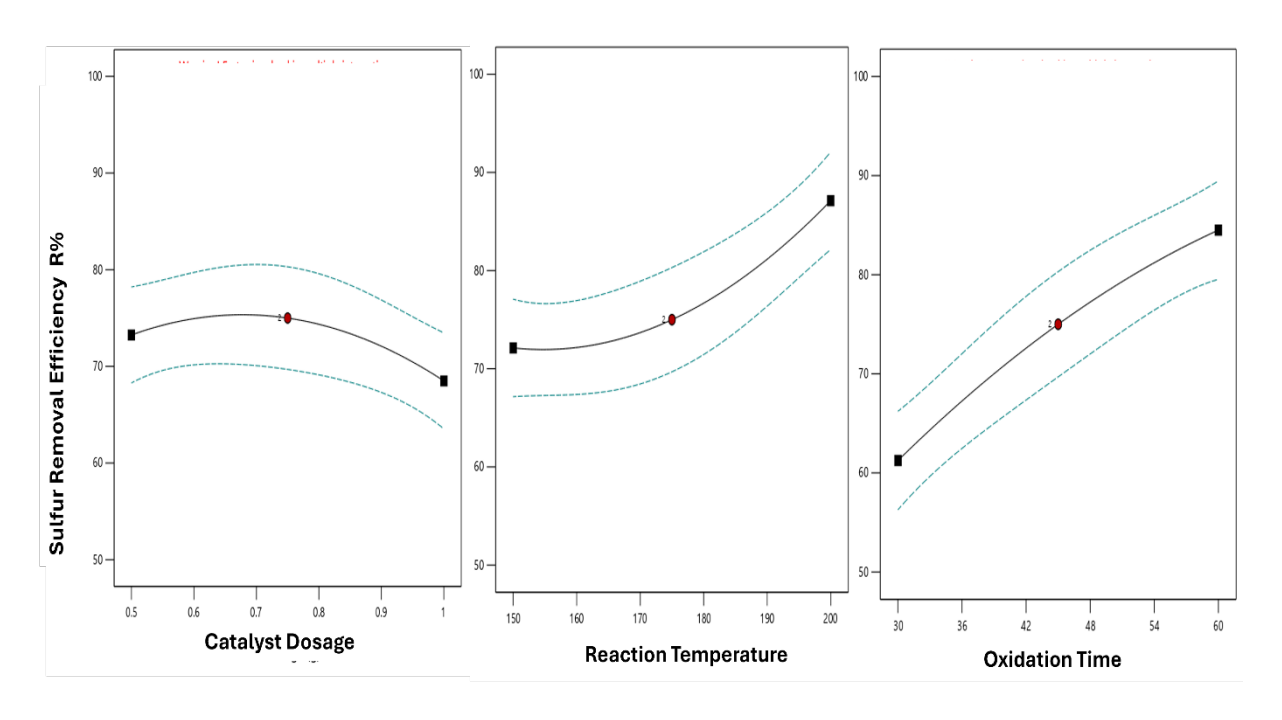


Figure 4. The effect of the studied variables individually on sulfur removal efficiency

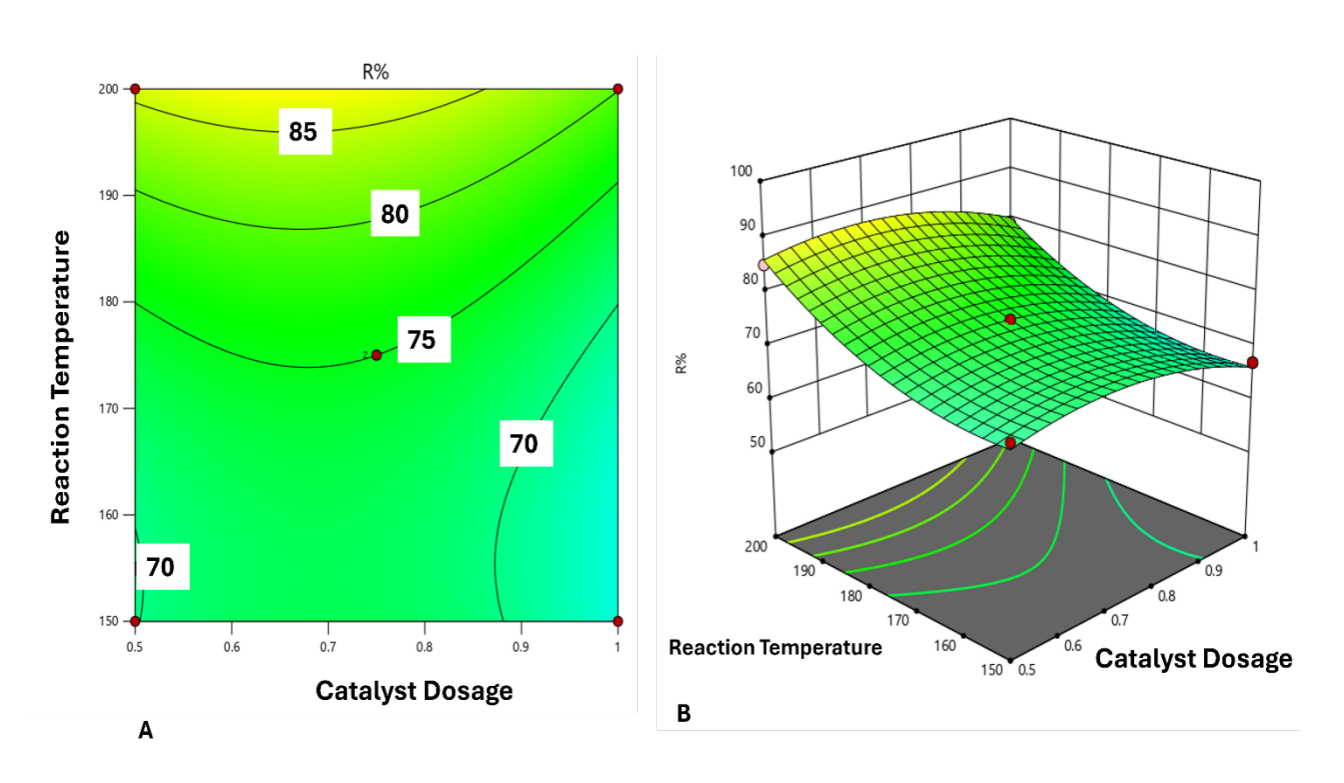


Figure 5. Interaction impact of the catalyst dosage, and reaction temperature on sulfur removal efficiency: A) contour plot, B) 3D

The interaction impact of the catalyst dosage and reaction temperature on sulfur removal efficacy is shown in **Figure 4**, the figure illustrates both the contour plot and the 3D, when the catalyst dosage is 0.5 g, the sulfur removal efficiency ranges from 70% (at 150 °C) to about 86% at 200 °C, but when the catalyst dosage is 1 g, and at the same range of reaction temperature (150-200)°C, the sulfur removal efficiency is between 65 to 80 %, as noted the impact of the catalyst amount is evident, even though temperature and time have a positive impact on the sulfur removal efficiency but the catalyst amount tendency to agglomerate when it was increased.

in which the efficiency is in the region of 80 - 90% (less than 90%), and this is due to the fact, as mentioned above, that the amount of the catalyst affects the decreasing sulfur removal efficiency. Similar behavior may be noted when studying the combined effect of both catalyst dosage and oxidation time, as seen in **Figure 5.** when the catalyst dosage is increased from 0.5 g to 1 g, the sulfur removal ranges from 63%- 84% with 0.5 g and 58%-78%, so it's again the catalyst dosage effect negatively on sulfur removal efficiency despite increasing time. The interaction effect of reaction temperature and oxidation time is shown on **Figure 6.** At 30 minutes, the sulfur removal efficiency ranges from 67% - 70% at 150 to 200 °C, while at 60 minutes, the sulfur removal efficiency rose from about 78% to about 99% at 150 to 200 °C. As seen, the maximum sulfur removal efficiency is shown at the upper-right corner (red area), where the sulfur removal efficiency is increased with the increase of time and temperature mentioned above [30, 33, 34].

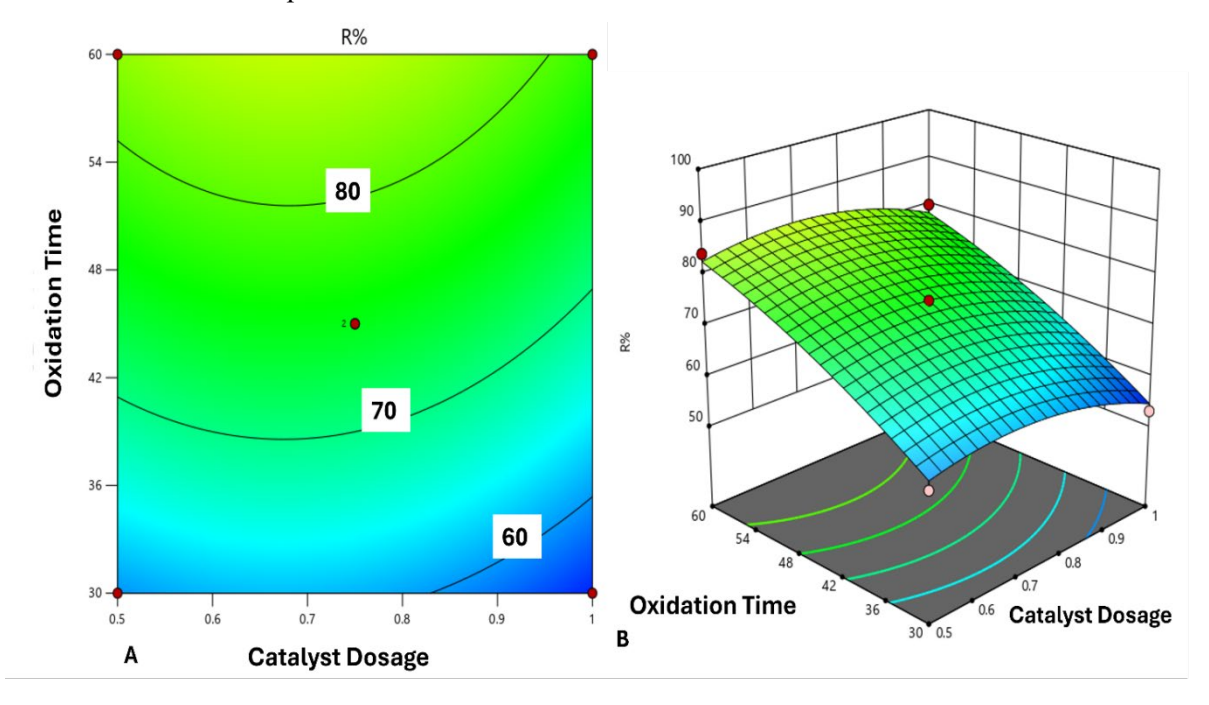


Figure 6. interaction impact of the catalyst dosage, and oxidation time on sulfur removal efficiency: A) contour plot, B) 3D

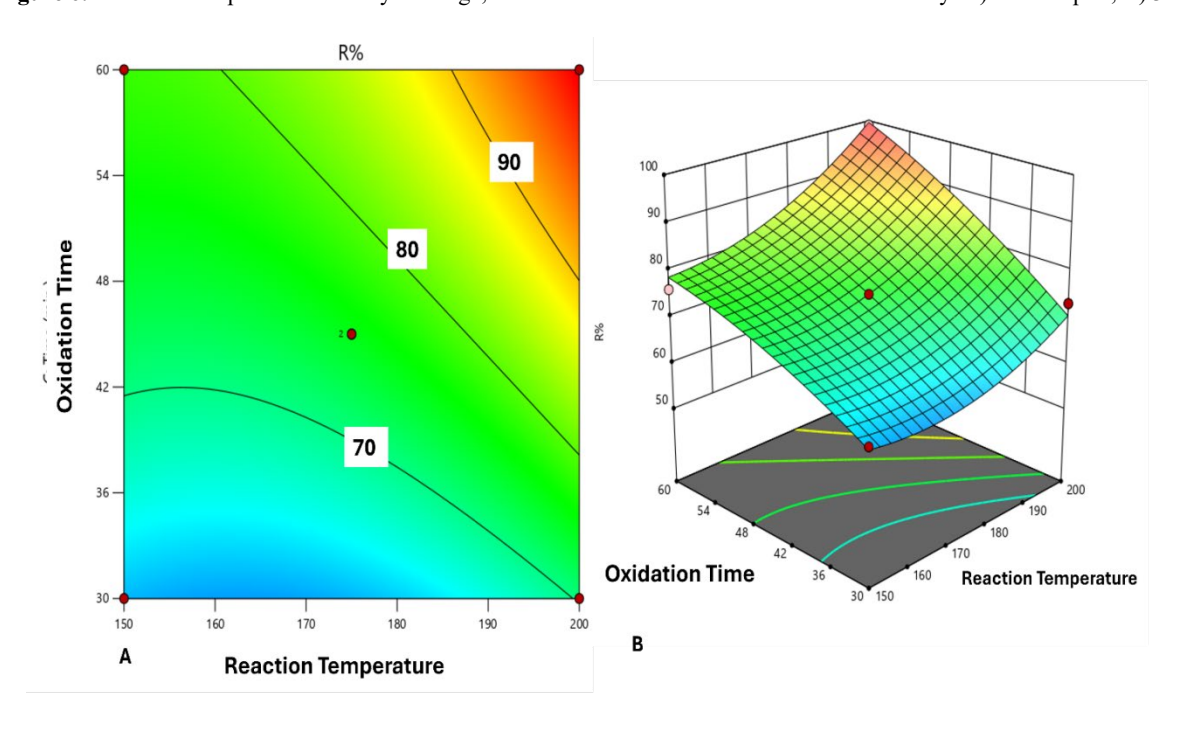


Figure 7. interaction impact of the oxidation time, and reaction temperature on sulfur removal efficiency: A) contour plot, B) 3D

5. Conclusion

In this study, the sulfur removal from gasoil by aerobic oxidative desulfurisation was investigated using a high entropy oxide catalyst as a new and active catalyst. Experimental design was conducted based on the Box-Behnken method with response surface methodology (RSM). The RSM was used to assess the impact of process variables and their interaction impact to accomplishing their optimum operating conditions. Under optimal operating conditions, including catalyst dosage 0.75 g, reaction temperature 200 °C, and oxidation time 60 minutes, the sulfur removal efficiency was found to be 98.12%. The experimental results reveal that sulfur removal efficiency is significantly enhanced by reaction temperature and oxidation time, while it's decreased with catalyst dosage

Acknowledgment

The authors would like to acknowledge Mr. Mohammed S. Fares / Quality control in State Electricity Production Company of Al-Furat Middle Region for his help in measuring sulfur content to support this research.

Conflict of interest

The authors declare no conflict of interest

References

- 1. A. Aghaei, S. Shahhosseini, and M. A. Sobati, "Regeneration of different extractive solvents for the oxidative desulfurization process: An experimental investigation," Process Safety and Environmental Protection, vol. 139, pp. 191–200, 2020, doi: https://doi.org/10.1016/j.psep.2020.04.013.
- 2. P. Zuo, Y. Liu, J. Jiao, J. Ren, R. Wang, and W. Jiao, "Ultrafine W2C well-dispersed on N-doped graphene: Extraordinary catalyst for ultrafast oxidative desulfurization of high sulfur liquid fuels," Appl Catal A Gen, vol. 643, p. 118791, 2022, doi: https://doi.org/10.1016/j.apcata.2022.118791.
- 3. H. Lü et al., "Deep catalytic oxidative desulfurization (ODS) of dibenzothiophene (DBT) with oxalate-based deep eutectic solvents (DESs)," Chemical Communications, vol. 51, no. 53, pp. 10703–10706, 2015, doi: 10.1039/C5CC03324A.
- 4. F. Vafaee, M. Jahangiri, and M. Salavati-Niasari, "A new phase transfer nanocatalyst NiFe2O4-PEG for removal of dibenzothiophene by an ultrasound assisted oxidative process: Kinetics, thermodynamic study and experimental design," RSC Adv, vol. 11, no. 50, pp. 31448–31459, Sep. 2021, doi: 10.1039/d1ra06751f.
- 5. L. Sun et al., "Aerobic oxidative desulfurization coupling of Co polyanion catalysts and p-TsOH-based deep eutectic solvents through a biomimetic approach," Green Chemistry, vol. 21, no. 10, pp. 2629–2634, 2019.
- 6. Z. Feng, Y. Zhu, Q. Zhou, Y. Wu, and T. Wu, "Magnetic WO3/Fe3O4 as catalyst for deep oxidative desulfurization of model oil," Materials Science and Engineering: B, vol. 240, pp. 85–91, 2019.
- 7. Y. Zhang, G. Ji, F. Ullah, and A. Li, "Polyoxometalate catalyzed oxidative desulfurization of diesel range distillates from waste tire pyrolysis oil," J Clean Prod, vol. 389, p. 136038, 2023.
- 8. E. Syntyhaki and D. Karonis, "Oxidative and extractive desulfurization of petroleum middle distillates, using imidazole ionic liquids," Fuel Communications, vol. 7, p. 100011, 2021, doi: https://doi.org/10.1016/j.jfueco.2021.100011.
- 9. E. Lucatero, R. Bashiri, and M. C. So, "Synthesis, Characterization, and Evaluation of Metal-Organic Frameworks for Oxidative Desulfurization: An Integrated Experiment," J Chem Educ, vol. 101, no. 8, pp. 3428–3433, Aug. 2024, doi: 10.1021/acs.jchemed.4c00297.
- 10. N. Li et al., "Oxidative desulfurization and magnetic properties of a mixed-valence cobalt vanadate," Polyhedron, vol. 226, p. 116077, 2022, doi: https://doi.org/10.1016/j.poly.2022.116077.
- 11. S. Jatav and V. C. Srivastava, "Ce/Al2O3 as an efficient catalyst for oxidative desulfurization of liquid fuel," Pet Sci Technol, vol. 37, no. 6, pp. 633–640, 2019.
- 12. H. H. Alwan, A. A. Ali, and H. F. Makki, "Optimization of Oxidative Desulfurization Reaction with Fe2O3 Catalyst Supported on Graphene Using Box-Behnken Experimental Method," 2020, doi: 10.9767/bcrec.15.1.6670.175.
- 13. H. J. Mohammed, A. T. Jarullah, B. A. Al-Tabbakh, and H. M. Hussein, "Preparation of synthetic composite nanocatalyst for oxidative desulfurization of kerosene," Energy Sources, Part A: Recovery, Utilization, and Environmental Effects, vol. 45, no. 1, pp. 1672–1685, 2023.
- 14. M. AbdulHassan and H. H. Alwan, "Boosting tungsten-based catalyst activity for aerobic oxidative desulfurization of gas oil by cerium," Results in Engineering, vol. 23, p. 102557, 2024.

- 15. H. Chen et al., "Mechanochemical Synthesis of High Entropy Oxide Materials under Ambient Conditions: Dispersion of Catalysts via Entropy Maximization," ACS Mater Lett, vol. 1, no. 1, pp. 83–88, Jul. 2019, doi: 10.1021/acsmaterialslett.9b00064.
- 16. H. Chen et al., "Self-regenerative noble metal catalysts supported on high-entropy oxides," Chemical Communications, vol. 56, no. 95, pp. 15056–15059, 2020, doi: 10.1039/D0CC05860B.
- 17. G. Cao et al., "Liquid metal for high-entropy alloy nanoparticles synthesis," Nature, vol. 619, no. 7968, pp. 73–77, 2023, doi: 10.1038/s41586-023-06082-9.
- 18. H. Lin et al., "High-entropy oxide based biomimetic catalysis system enables robust oxidative desulfurization with an excellent regeneration ability," Sep Purif Technol, vol. 348, p. 127729, 2024, doi: https://doi.org/10.1016/j.seppur.2024.127729.
- 19. S. Ahmadzadeh, A. Asadipour, M. Pournamdari, B. Behnam, H. R. Rahimi, and M. Dolatabadi, "Removal of ciprofloxacin from hospital wastewater using electrocoagulation technique by aluminum electrode: Optimization and modelling through response surface methodology," Process Safety and Environmental Protection, vol. 109, pp. 538–547, 2017, doi: https://doi.org/10.1016/j.psep.2017.04.026.
- 20. M. S. Tizo et al., "Efficiency of calcium carbonate from eggshells as an adsorbent for cadmium removal in aqueous solution," Sustainable Environment Research, vol. 28, no. 6, pp. 326–332, 2018.
- 21. F. H. Hussein, A. F. Halbus, A. J. Lafta, and Z. H. Athab, "Preparation and characterization of activated carbon from iraqi khestawy date palm," J Chem, vol. 2015, 2015, doi: 10.1155/2015/295748.
- 22. H. Xu et al., "Preparation method of Co3O4 nanoparticles using degreasing cotton and their electrochemical performances in supercapacitors," J Nanomater, vol. 2014, no. 1, p. 723057, 2014.
- 23. M. K. Trivedi et al., "Characterization of physical, thermal and structural properties of chromium (VI) oxide powder: Impact of biofield treatment," Powder Metallurgy & Mining, vol. 4, no. 1, 2015.
- 24. N. A. Jawad and K. H. Hassan, "Structural characterization of NiO nanoparticles prepared by green chemistry synthesis using arundo donaxi leaves extract," in Journal of Physics: Conference Series, IOP Publishing, 2021, p. 012007.
- 25. K. Deori and S. Deka, "Morphology oriented surfactant dependent CoO and reaction time dependent Co 3 O 4 nanocrystals from single synthesis method and their optical and magnetic properties," CrystEngComm, vol. 15, no. 42, pp. 8465–8474, 2013.
- W. G. Adnan and A. M. Mohammed, "Green synthesis of chromium oxide nanoparticles for anticancer, antioxidant and antibacterial activities," Inorg Chem Commun, vol. 159, p. 111683, 2024, doi: https://doi.org/10.1016/j.inoche.2023.111683.
- 27. H. H. Alwan, A. A. Abd, H. F. Makki, and M. R. Othman, "Optimizing hydrodesulfurization of naphtha using NiMo/graphene catalyst," Journal of Industrial and Engineering Chemistry, 2024.
- 28. M. A. Alheety, S. A. Al-Jibori, A. Karadağ, H. Akbaş, and M. H. Ahmed, "A novel synthesis of MnO2, nanoflowers as an efficient heterogeneous catalyst for oxidative desulfurization of thiophenes," Nano-Structures & Nano-Objects, vol. 20, p. 100392, 2019, doi: https://doi.org/10.1016/j.nanoso.2019.100392.
- 29. Y. Shu, J. Bao, S. Yang, X. Duan, and P. Zhang, "Entropy-stabilized metal-CeOx solid solutions for catalytic combustion of volatile organic compounds," AIChE Journal, vol. 67, no. 1, p. e17046, 2021.
- 30. J. I. Humadi and W. T. Mohammed, "Fast, ultradeep, and continuous desulfurization of heavy gasoil in novel oscillatory basket central baffled reactor using MnO2-incorparted Fe2O3- supported activated carbon catalyst," Fuel, vol. 400, Nov. 2025, doi: 10.1016/j.fuel.2025.135716.
- 31. T. A. Saleh, K. O. Sulaiman, S. A. AL-Hammadi, H. Dafalla, and G. I. Danmaliki, "Adsorptive desulfurization of thiophene, benzothiophene and dibenzothiophene over activated carbon manganese oxide nanocomposite: with column system evaluation," J Clean Prod, vol. 154, pp. 401–412, 2017, doi: https://doi.org/10.1016/j.jclepro.2017.03.169.
- 32. S. Murata, K. Murata, K. Kidena, and M. Nomura, "A novel oxidative desulfurization system for diesel fuels with molecular oxygen in the presence of cobalt catalysts and aldehydes," Energy & fuels, vol. 18, no. 1, pp. 116–121, 2004
- 33. J. Zhang, J. Li, T. Ren, Y. Hu, J. Ge, and D. Zhao, "Oxidative desulfurization of dibenzothiophene based on air and cobalt phthalocyanine in an ionic liquid," RSC Adv, vol. 4, no. 7, pp. 3206–3210, 2014, doi: 10.1039/C3RA43765E.
- 34. M. A. Alheety, S. A. Al-Jibori, A. Karadağ, H. Akbaş, and M. H. Ahmed, "A novel synthesis of MnO2, nanoflowers as an efficient heterogeneous catalyst for oxidative desulfurization of thiophenes," Nano-Structures & Nano-Objects, vol. 20, p. 100392, 2019, doi: https://doi.org/10.1016/j.nanoso.2019.100392.
- 35. I. Mohammed, H. H. Alwan, and A. N. Ghanim, "Using Box-Behnken experimental design for optimization of gas oil desulfurization by electrochemical oxidation technique," in IOP Conference Series: Materials Science and Engineering, IOP Publishing Ltd, Nov. 2020. doi: 10.1088/1757-899X/928/2/022158.